PAGEOPH, Vol. 136, No. 1 (1991) 0033–4553/91/010103–24$1.50 + 0.20/0

Single-station Estimates of the Seismic Moment of the 1960 Chilean and 1964 Alaskan Earthquakes, Using the Mantle Magnitude M_m

EMILE A. OKAL[1] and JACQUES TALANDIER[2]

Abstract—Measurements are taken of the mantle magnitude M_m, developed and introduced in previous papers, in the case of the 1960 Chilean and 1964 Alaskan earthquakes, by far the largest events ever recorded instrumentally. We show that the M_m algorithm recovers the seismic moment of these gigantic earthquakes with an accuracy (typically 0.2 to 0.3 units of magnitude, or a factor of 1.5 to 2 on the seismic moment) comparable to that achieved on modern, digital, datasets. In particular, this study proves that the mantle magnitude M_m does not saturate for large events, as do standard magnitude scales, but rather keeps growing with seismic moment, even for the very largest earthquakes. We further prove that the algorithm can be applied in unfavorable experimental conditions, such as instruments with poor response at mantle periods, seismograms clipped due to limited recording dynamics, or even on microbarograph records of air coupled Rayleigh waves.

In addition, we show that it is feasible to use acoustic-gravity air waves generated by those very largest earthquakes, to obtain an estimate of the seismic moment of the event along the general philosophy of the magnitude concept: a single-station measurement ignoring the details of the earthquake's focal mechanism and exact depth.

Key words: Seismic sources, magnitudes, large earthquakes, acoustic-gravity waves.

Introduction and Purpose

The purpose of this paper is to test the variable-period mantle magnitude M_m in the case of gigantic earthquakes for which standard magnitudes, affected by total saturation, fail to provide an adequate estimate of the true size of the event. The concept of M_m was introducted by OKAL and TALANDIER (1989; hereafter Paper I), as a means of retrieving in real time an estimate of the seismic moment M_0 of an earthquake while keeping the general concept of a *magnitude* scale, i.e., a quick, one-station measurement not requiring the knowledge of the event's focal mechanism or exact depth. The mantle magnitude M_m, initially developed on Rayleigh

[1] Department of Geological Sciences, Northwestern University, Evanston, Illinois 60208, USA.
[2] Laboratoire de Détection et Géophysique and Centre Polynésien de Prévention des Tsunamis, Commissariat à l'Energie Atomique, Boîte Postale 640, Papeete, Tahiti, French Polynesia.

waves, was later extended to Love waves by OKAL and TALANDIER (1990; hereafter Paper II). We refer to Papers I and II for the theoretical justification of the expression

$$M_m = \log_{10} X(\omega) + C_D + C_S - 0.90 \tag{1}$$

where $X(\omega)$ is the spectral amplitude (expressed in μm-s) of ground displacement at the angular frequency ω, and C_D and C_S frequency-dependent corrections for distance and source excitation effects, respectively. The "locking" constant -0.90 in (1) theoretically predicts that M_m should be an estimate of $[\log_{10} M_0 - 20]$, where M_0 is in dyn-cm. We also showed in Paper I, and justified in OKAL (1989), that a direct time-domain measurement on a Rayleigh wave record low-pass-filtered at 25 mHz was possible, using the expression

$$M_m^{TD} = \log_{10} [A \cdot T] + C_S + C_D - 1.20 \tag{2}$$

where A is the zero-to-peak amplitude of an oscillation of the signal (in microns), of apparent period T. At large distances Δ, an additional term $0.5 \log_{10} \Delta/70^\circ$ must be added to the correction C_D, to reflect the increasingly dispersed character of the mantle Rayleigh wave. This correction becomes significant for $\Delta > 120^\circ$.

Our main objective in developing M_m was to build a magnitude scale avoiding the well-known saturation effects which plague any scale measured at a constant period (GELLER, 1976). In particular, total saturation around $M_s = 8.3$ renders the standard 20-s surface wave magnitude M_s (which GELLER and KANAMORI (1977) have shown to be identical to the "Richter" scale used by GUTENBERG and RICHTER (1954) to estimate many large historical events) useless for the study of the very largest earthquakes. The use of M_s becomes outright dangerous in the context of tsunami warning and prevention, given that the scale starts saturating at just about the moment level (10^{28} dyn-cm) where tsunami generation becomes non-trivial, and therefore cannot provide any reliable quantitative estimate of the tsunamigenic character of an event. Conversely, the mantle magnitude M_m was integrated into an automated real-time tsunami detection algorithm (TALANDIER and OKAL, 1989).

Through a series of performance tests on data sets of more than 500 records, we showed in Papers I and II that M_m is not affected by saturation and keeps growing as $\log_{10} M_0$. The slopes of best-fitting straight lines regressing the logarithm of published M_0 values as a function of measured M_m were not significantly different from 1, between M_m values of 6 and 8.4. Later, REYMOND *et al.* (1991) have shown that the method can be extended to lower moment ranges ($M_m \geq 3.9$) without difficulty or loss of performance. However, we were limited in our previous studies by the desire to keep a homogeneous, mostly digital, data set for which reliable moment values are available, for example from the CMT solutions published by DZIEWONSKI *et al.* (1983; and subsequent quarterly updates). However, the ultimate test of the validity of the M_m concept will be its ability to recognize in

real-time a gigantic event carrying extreme tsunami hazard. At the time of writing (May 18, 1991), there has not been a truly gigantic earthquake ($M_0 \geqslant 10^{29}$ dyn-cm) for 26 years (since the 4 February 1965 Rat Island earthquake), and thus no such earthquake was included in the data sets analyzed in Papers I and II. The purpose of the present study is to test the performance of M_m on the two largest events ever recorded instrumentally: the 1960 Chilean and 1964 Alaskan earthquakes.

We want to emphasize that our goal in the present study is not to analyze every single available seismogram for either of the events, but rather to show on a number of examples, some of them purposely selected so as to involve inferior instrumentation and geometry, that M_m does recover a reasonable estimate of the moments. We will also show that an estimate of the seismic moment can be derived from microbarograph records of the acoustic-gravity waves generated by the events.

Seismic Waves: The 1964 Alaskan Event

At the time of the 1964 Alaskan earthquake, the WWSSN had been deployed, and a set of excellent records is available, which incidentally, formed the backbone of the first comprehensive investigation of the earth's normal modes (DZIEWONSKI and GILBERT, 1972). The source process of the event itself was investigated by KANAMORI (1970) who obtained a moment $M_0 = 7.5 \times 10^{29}$ dyn-cm, and later revised the figure to 8.2×10^{29} (KANAMORI, 1977). We will use the latter figure as a reference moment, which we will write as equivalent to a "published mantle magnitude" $M_m^p = \log_{10} M_0 - 20 = 9.91$.

In the case of the Alaskan event, our goal is to show that, despite the absence of broadband instrumentation, the M_m algorithm can be successfully applied to available records, even under conditions of inadequate geometries or instrumentation. For this purpose, we used three kinds of records:

Individual WWSSN Long-period Records

Since the moment of the event was derived precisely from a set of WWSSN records (KANAMORI, 1970), we will simply show that an estimate of M_0 can be obtained from an individual record. For this purpose, we selected the vertical long-period instrument at Mundaring (MUN), and processed its phases R_3 and R_5. The resulting M_m values are 9.48 and 9.42, respectively. These digitized records are shown on Figure 1, and all relevant information listed in Table 1. Following the procedure in Paper I, we also computed a "corrected" value, M_c, to estimate what fraction of the residuals $r = M_m - M_m^p$ is due to the systematic error involved in correcting for an average focal mechanism and depth, rather than for the exact ones

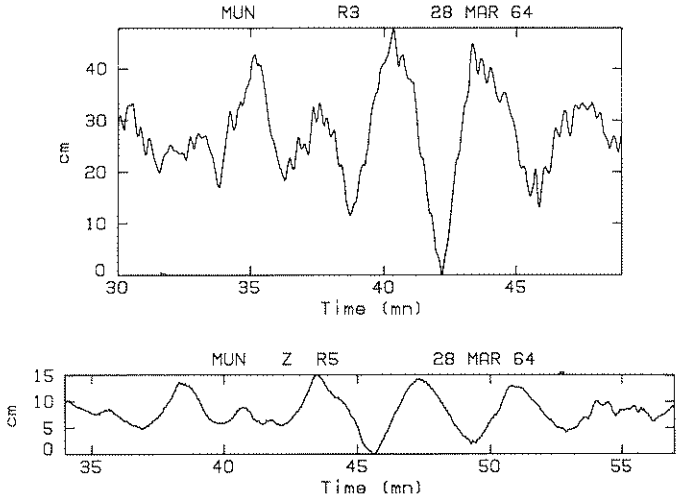

Figure 1
Vertical WWSSN 30–100 records of the 1964 Alaskan earthquake at Mundaring. Plotted are the third and fifth passages of the Rayleigh wave. The records have been equalized to a standard magnification of 1500. Note the spectacular amplitudes.

Table 1

Summary of results for the 1964 Alaskan Earthquake
$M_m^p = 9.91$ (KANAMORI, 1977)

Station	Code	Instrument	Wavetrain	Distance (°)	M_m	Period (s)	M_c
			Frequency domain measurements				
Mundaring	MUN	WWSSN 30–100	R_3	480.36	9.48	293	9.61
Mundaring	MUN	WWSSN 30–100	R_5	840.36	9.42	256	9.58
Uppsala	UPP	Wiechert	G_2	306.72	9.57	256	9.59
Uppsala	UPP	Wiechert	G_4	666.72	9.45	256	9.48
Papeete	PPT	Microbarograph	R_1	78.4	9.87	123	9.70
			Time domain measurements				
Papeete	PPT	Microbarograph	R_1	78.4	9.90	162	9.73

published by KANAMORI (1970). The remaining deficiency in M_c, characterized by the residuals $r_c = M_c - M_m^p = -0.22$ and -0.25 respectively, is probably due to a source finiteness effect: the size of the earthquake is such that even at the longest periods recorded on the WWSSN instruments, the amplitude of the wave is slightly affected by directivity. At any rate, the values obtained for r_c are typical of the scatter achieved when using modern data (see Paper I, Table 6).

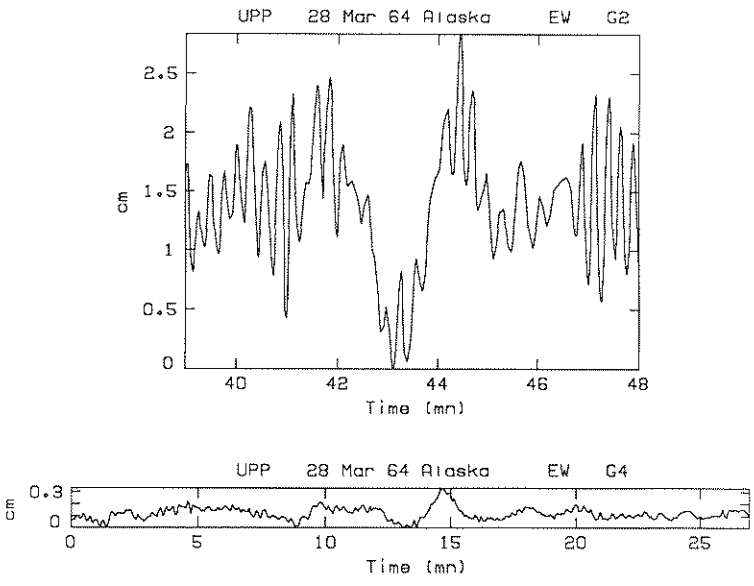

Figure 2
Wiechert records of the 1964 Alaskan earthquake at Uppsala. Plotted are the second and fourth passages of the Love wave, as recorded on the East-West component. Note that the two plots have different time scales.

Wiechert Records at Uppsala

We also include in the present study records obtained at Uppsala (UPP) as part of a more general study of historical seismograms (OKAL, 1991). Only the East-West component (mostly Love polarization) was of high enough quality to be used. Figure 2 shows the phases G_2 and G_4 which yielded $M_m = 9.57$ and 9.45 respectively. Corrected values would be $M_c = 9.59$ and 9.48. These values are somewhat deficient, which is an illustration of the fact that the enormous length of propagation of the rupture would probably require measurements at periods beyond 300 s, for which the instrument response is significantly degraded. Nevertheless, the earthquake is clearly identified as gigantic.

Microbarograph Record of Rayleigh Waves in Polynesia

A long-period seismometer did operate at the Papeete Geophysical Laboratory (PPT) in 1964. However, the emphasis at the time was on short-period surface waves (around 20 s period), using sharply selective narrow-band-pass filters reducing the magnification of the instrument at mantle periods. As a result, the PPT record cannot be used for an M_m computation. However, two microbarographs were operating at Papeete (PPT) and Bora-Bora (16.44°S; 151.75°W), providing usable records of an air wave ground-coupled to the mantle Rayleigh wave. Such

records, recognized originally by BENIOFF *et al.* (1951), amount to a detection of the Rayleigh wave through its weak continuation into the atmosphere. In the case of the 1964 Alaskan earthquake, BOLT (1964) and DONN and POSMENTIER (1964) have published and discussed such signals, mostly from the standpoint of the dispersion of the Rayleigh wave, without attempting to quantify the source directly from the amplitude of the recorded overpressure. More generally, YUEN *et al.* (1969) have shown on the example of the 1968 Tokachi-Oki earthquake that a Rayleigh wave's "tail" into the atmosphere can be detected at altitudes as high as 300 km, from the oscillations it induces onto the ionosphere.

The spectral amplitude $P(\omega)$ of the overpressure signal at the air-ground interface can be converted to the vertical displacement spectrum $X(\omega)$ of the Rayleigh wave by the relation

$$P(\omega) = \rho c_{\text{atm.}} V(\omega) = \rho c_{\text{atm.}} \omega X(\omega) \tag{3}$$

where $\rho = 1.2\ \text{kg/m}^3$ and $c_{\text{atm.}} = 331\ \text{m/s}$ are the atmosphere's density and sound velocity at zero altitude, and $V(\omega)$ is the amplitude spectrum of the vertical particle velocity of the free surface. This equation is valid in the limit $c/c_{\text{atm.}} \gg 1$, where c is the Rayleigh wave's phase velocity (HASKELL, 1951). Furthermore, for a Rayleigh wave at mantle periods, the vertical displacement at the surface is not affected significantly by the presence of the ocean column. Thus microbarographs, which have a practically flat response well into the mantle wave frequency band, would be equivalent to velocity sensors, or in other words to seismometers with a ω^{-1} response fall-off at long periods. In order to improve the signal-to-noise ratio, the two records at Papeete and Bora-Bora were stacked after time-lagging by cross-correlation (Figure 3a), then deconvolved for vertical ground motion and filtered (Figures 3b, c), and estimates of M_m computed both in the time and frequency domains. Results are included in Table 1. In practice, the instrument recovers the moment flawlessly: $M_m = 9.87$ in the frequency domain, 9.90 in the time domain.

In conclusion, in the case of the Alaskan earthquake, the four values of M_m measured from standard seismometers have an average residual $\bar{r} = -0.43$ and a standard deviation $\sigma = 0.07$. These numbers are relative to the revised estimate $M_m^p = 9.91$ (KANAMORI, 1977). While these residuals are large, they are in part due to the systematic error involved in using C_S, rather than the exact focal mechanism. Values for the corrected magnitudes would be $\bar{r}_c = -0.31$; $\sigma_c = 0.02$. The generally negative character of these residuals reflects the extreme duration of the source, which would require measurements outside the range of performance of standard instruments. If the residuals are computed with respect to KANAMORI'S (1970) original estimate ($M_m = 9.87$), they improve slightly and the new value of $\bar{r}_c$ (-0.27) is within the 1-σ scatter of the extensive data sets studied in Papers I and II. At any rate, the exceptional size of the event is recovered beyond doubt. With its broader response, the microbarograph performs even better.

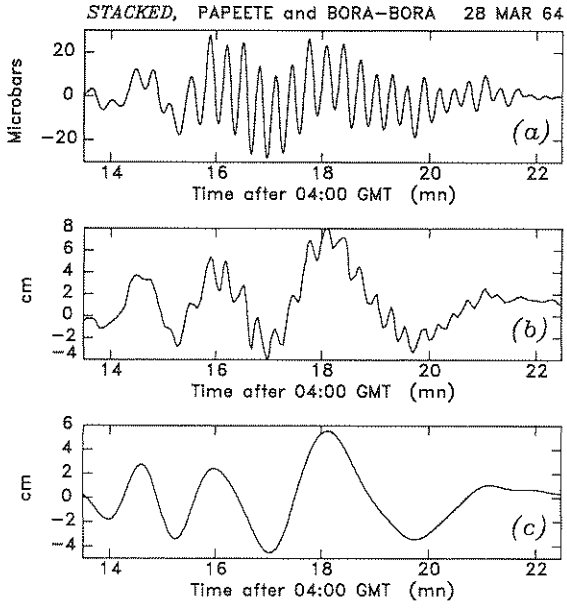

Figure 3
Microbarograph records of Rayleigh waves from the 1964 Alaskan earthquake. (a): Original pressure signal, stacked at Papeete and Bora-Bora. (b): Vertical ground motion deconvolved from (a) in the period range 12–600 s for use in the frequency domain analysis. (c): Vertical ground motion further filtered in the period range 50–400 s, for use in the time-domain analysis.

Seismic Waves: The 1960 Chilean Event

This earthquake has long been recognized as the largest event ever recorded instrumentally. The first estimate of its moment can be reconstructed from BEN-MENAHEM'S (1971) "source constant" $\Omega = 2$ mm, equivalent to $M_0/4\pi\mu a^2$ where a is the radius of the earth and μ the rigidity of the source medium, and translating into $M_0 = 1.6 \times 10^{30}$ dyn-cm. In the definitive study on this earthquake's geometry, KANAMORI and CIPAR (1974) proposed a value of 2×10^{30} dyn-cm for the main shock of the event, and indicated that the total seismic release, including the slow precursor, could amount to as much as 6×10^{30} dyn-cm. The analysis of interference patterns among the earth's free oscillations by KANAMORI and ANDERSON (1975) suggested a moment of $(3-4) \times 10^{30}$ dyn-cm. GELLER (1977) confirmed a total value of 2.4×10^{30} dyn-cm based on the excitation of the gravest mode of the earth ${}_0S_2$. More recently, CIFUENTES and SILVER (1989) analyzed an extensive data set of the event's normal modes, as recorded on the Press-Ewing instruments deployed during the IGY, and came up with figures of 3.2×10^{30} dyn-cm for the main shock, starting around 19:09 GMT on May 22 and lasting approximately 3 mn, with a total release of 5.5×10^{30} dyn-cm spread over 25 mn, starting at

18:52 GMT. We will use their figure for the mainshock as the published reference for this event; it would be illusory to attempt to retrieve the slow component of seismic moment release from a single wavetrain. We will write this in the form an equivalent published M_m, or $M_m^P = 10.51$.

Records Analyzed

Since the 1960 Chilean event predates the WWSSN, we analyzed several types of records obtained on a variety of instruments. Results are regrouped in Table 2.

Table 2

Summary of results for the 1960 Chilean Earthquake
$M_m^P = 10.51$ (CIFUENTES and SILVER, 1989)

Station	Code	Instrument	Wavetrain	Distance (°)	M_m	Period (s)	M_c
			Frequency domain measurements M_m				
Uppsala	UPP	Wiechert	G_2	235.75	9.64	256	9.81
Uppsala	UPP	Wiechert	R_2	235.75	9.67	171	9.91
Uppsala	UPP	Wiechert	R_4	595.75	9.74	228	9.93
Seven Falls	SFA	Wood-Anderson	G_4	634.54	10.29	142	10.77
Palisades	PAL	Press-Ewing	R_4	640.68	9.86	233	10.19
Palisades	PAL	Press-Ewing	R_6	1000.68	9.79	233	10.13
Palisades	PAL	Press-Ewing	R_8	1360.68	10.16	122	10.68
Resolute	RES	Press-Ewing	G_6	966.07	10.13	142	10.45
Resolute	RES	Press-Ewing	G_8	1326.07	10.24	213	10.57
Resolute	RES	Press-Ewing	G_{10}	1686.07	10.17	183	10.50
Resolute	RES	Press-Ewing (Z)	R_{10}	1686.07	10.18	171	10.55
Resolute	RES	Press-Ewing (NS)	R_{10}	1686.07	10.57	213	10.88
Pasadena	PAS	180-s Strainmeter	G_2	276.53	9.77	284	10.02
Pasadena	PAS	180-s Strainmeter	G_4	636.53	9.78	284	10.03
Pasadena	PAS	180-s Strainmeter	R_2	276.53	9.99	233	10.16
Pasadena	PAS	180-s Strainmeter	R_4	636.53	10.05	284	10.20
La Folinière	FLN	LDG-Long Period	R_4	611.62	10.22	205	10.45
La Folinière	FLN	LDG-Long Period	R_5	828.38	9.82	246	10.05
La Folinière	FLN	LDG-Long Period	R_6	971.62	10.31	223	10.54
La Folinière	FLN	LDG-Long Period	G_4	611.62	10.07	205	10.24
La Folinière	FLN	LDG-Long Period	G_5	828.38	9.67	223	9.82
La Folinière	FLN	LDG-Long Period	G_6	971.62	10.33	205	10.50
La Folinière	FLN	LDG-Long Period	G_7	1188.38	10.08	246	10.23
			Time domain measurements M_m^{TD}				
La Folinière	FLN	LDG-Long Period	R_4	611.62	10.32	226	10.55
La Folinière	FLN	LDG-Long Period	R_5	828.38	9.94	269	10.27
La Folinière	FLN	LDG-Long Period	R_6	971.62	10.44	245	10.67

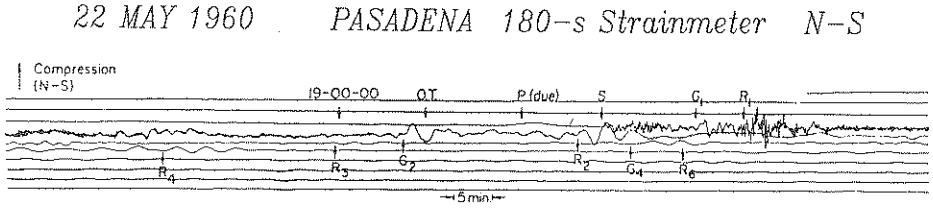

Figure 4
Pasadena record of the 1960 Chilean earthquake on the low-gain, 180-s strainmeter. The wavetrains G_2, R_2, G_4 and R_4 were used in this study. After KANAMORI and CIPAR (1974).

Pasadena Strainmeter. We processed the famous record on the North-South low-gain strainmeter at Pasadena, previously used by BEN-MENAHEM (1971) and KANAMORI and CIPAR (1974), and reproduced in Figure 4. Targeted were the dominant phases R_2, G_2, R_4 and G_4. The response of the instrument was studied in detail by KANAMORI and CIPAR (1974), who concluded that it is equivalent to that a mechanical seismograph with constants $T = 180$ s, $V = 10$, $h = 4$.

IGY Press-Ewing Network. During the International Geophysical Year, Press-Ewing instruments which were to become the prototypes of the long-period WWSSN, were deployed at a dozen sites worldwide. These records provided the bulk of the data from which the early analyses of the earth's normal modes were performed. Their responses have been compiled most recently by CIFUENTES and SILVER (1989). We concentrated on the Palisades and Resolute records, obtained from the Lamont-Doherty Geological Observatory archives (see Figure 5 for sample wavetrains).

Uppsala Wiechert and Seven Falls Records. We include in our data set 3 wavetrains obtained on the Uppsala Wiechert (KULHÁNEK, 1987), as part of our concurrent systematic study of the application of M_m to historical earthquakes (OKAL, 1991). We also include a record of G_2 at Seven Falls, obtained on a torsion seismometer.

Narrow-band Long-period Records

Records of the Chilean event at La Folinière, France (48.76°N, 0.48°W; Code FLN) were recently discovered in the archives of the Geophysical Laboratory of Commissariat à l'Energie Atomique in Paris. These instruments had a response roughly comparable to that of a standard electromagnetic system with a maximum magnification around 20 s. In particular, the narrowband filters later developed to boost the 20-s amplification (see above discussion of the Alaska event) were not available in 1960, and therefore the response of the instrument follows the straight ω^3 fall-off characteristic of standard electromagnetic seismographs. The paper chart recordings had only limited dynamic range, resulting in severe clipping even for

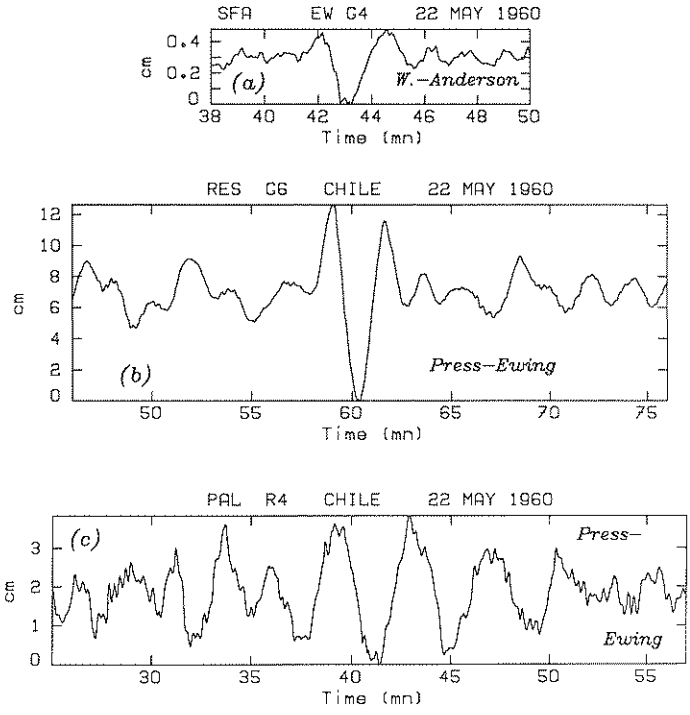

Figure 5
Examples of conventional records of the 1960 Chilean earthquake. (a): G_4 at Seven Falls, Québec (Wood-Anderson instrument); (b): G_6 at Resolute (IGY Press-Ewing); (c): R_4 at Palisades (Press-Ewing). Note difference in time and amplitude scales.

multiple passages (see Figure 6), entirely due to the mechanical characteristics of the paper recording, rather to the seismograph itself. We corrected for clipping by considering each clipped arch and least-squares fitting a half-sinusoid through the undisturbed points. The resulting seismogram was then analyzed both in the time and frequency domains.

Results

The most fundamental result is that the average measured M_m is 10.02, with the smallest value being 9.64 (G_2 at Uppsala). This means that the M_m algorithm positively recognizes the Chilean earthquake as the gigantic event it truly is, unparalleled ever since the dawn of seismic recording. Indeed, our concurrent systematic study applying M_m to large data sets of historical records (OKAL, 1991) has failed to come up with any comparable measurements: the 1960 Chilean and 1964 Alaskan earthquakes stand alone as the only events beyond $M_m = 9.5$. Furthermore, M_m correctly ranks the Chilean event above the Alaskan one. In this

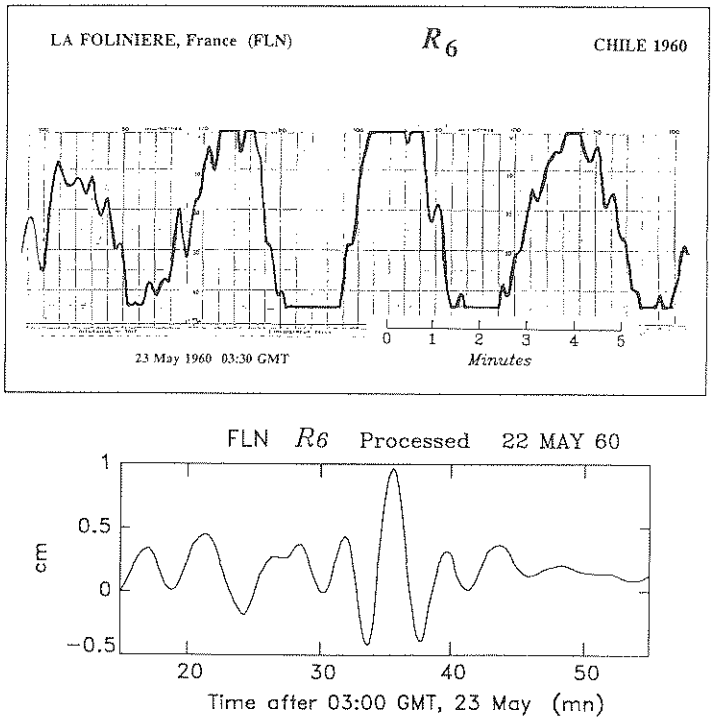

Figure 6
Sixth Rayleigh passage (R_6) observed at La Folinière, France on the LDG narrow-band long-period instrument. *Top:* 15-minute portion of the original signal, showing severe clipping due to limited dynamical range of the paper chart recorder. *Bottom:* Processed signal representing ground motion (reaching 1.5 cm peak-to-peak) after reconstruction to elimate clipping, filtering out for $T \geqslant 100$ s, and removal of instrument response.

respect, it performs better than BRUNE and ENGEN'S (1969) 100-s magnitude M_{100}; the latter, conceptually close to M_m but measured at a fixed period $T = 100$ s, could not avoid eventual saturation for gigantic earthquakes, and ranked Alaska larger than Chile.

At this point, on the basis of both the Chilean and Alaskan results, we can affirm that M_m has successfully achieved its goal, as presented in Paper I, of avoiding saturation effects, even for the very largest earthquakes, while at the same time retaining the simple concept of a magnitude scale.

The average value of the residual $\bar{r}$ is -0.49, with $\sigma = 0.26$. While this number looks large, it must be emphasized that most stations used suffered from an unfavorable focal geometry. Indeed, the average corrected residual, $\bar{r}_c$ is only -0.22. Furthermore, all residuals are computed with respect to CIFUENTES and SILVER'S (1989) value of the moment of the main shock; the residuals would be smaller if referred to the earlier, and lower estimate of KANAMORI and CIPAR (1974). Not surprisingly, the best results are obtained on the IGY Press-Ewing

instruments, which feature improved magnification well into the longest mantle periods. For this subset, $\bar{r} = -0.37$; $\bar{r}_c = -0.02$. Among other instruments, the torsion seismometer at Seven Falls is one of the best performers, while the Uppsala Wiechert yields consistently deficient amplitudes.

We also demonstrate that time-domain measurements can be extended to very large events. Results at FLN show a general deficiency for odd passages, which is attributable to a remnant of directivity, even at the very large periods used; however the joint use of odd and even passages guards against significant underestimation of the source. These records also uphold the use the additional correction $0.5 \log_{10} [\Delta/70^\circ]$ for multiple passages.

Acoustic-gravity Waves

We investigate here the possibility of using acoustic-gravity waves recorded on microbarographs to quantify the source of the Alaskan and Chilean earthquakes. As opposed to the case previously studied, in which we were detecting the Rayleigh wave through its weak continuation into the atmosphere, we will now study a truly atmospheric acoustic or gravity wave, generated through the excitation by the buried source of its weak continuation into the solid earth. That the eigenfunction is weakly continued into the solid earth also allowed RITSEMA (1980) to detect this type of wave using a standard long-period seismometer, following the explosion of Mount St. Helens on 18 May 1980.

Data: 1964 Alaskan Earthquake

In the case of the Alaskan earthquake, we use the Berkeley (BKS) and East San Diego (ESD) records published by MIKUMO (1968). This author forward-modeled the excitation of atmospheric waves by the Alaskan earthquake using as an intermediate step the ground strong motion in the epicentral region in order to compute the excitation of the atmosphere. We will show that the spectral amplitude of these records can provide an excellent estimate of the seismic moment of the event.

The original records, digitized from MIKUMO (1968) are shown on Figure 7. MIKUMO also provides instrument response information (his Table 1 and Figure 9), even though it is not exactly clear at which frequency the sensitivity of the microbarographs is given. We take it to represent the gain at the period of maximum sensitivity. It is immediately apparent that these records are characterized by abundant very long-period energy, especially in the 400–700 s range, arriving at a group velocity of approximately 310 m/s. The combination of these properties identifies the wave as being the fundamental gravity mode GR_0 (PRESS and HARKRIDER, 1962). However, this mode can be contaminated by the acoustic

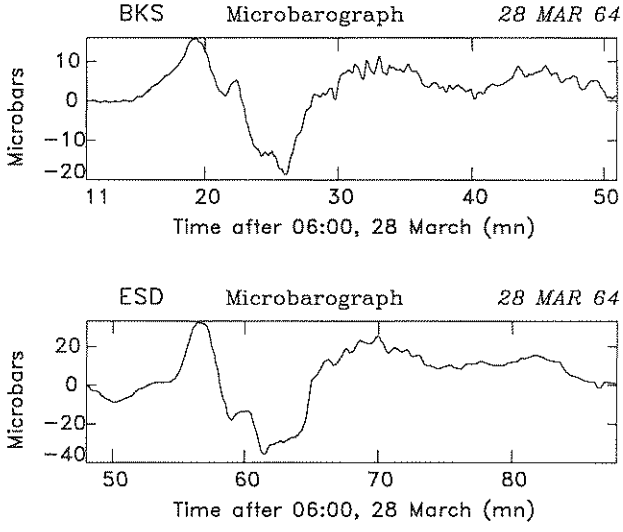

Figure 7
GR_0 gravity wave records of the 1964 Alaskan earthquake at Berkeley (BKS, *Top*) and East San Diego (ESD, *Bottom*), as digitized from MIKUMO (1968). Note different vertical scales.

branch S_0 in the range 360–420 s. For this reason, we will restrict our investigation to $T = 500-700$ s. Table 3 gives spectral amplitudes at two Fourier periods (512 and 640 s) for both BKS and ESD.

Data: 1960 Chilean Earthquake

While no seismic stations were run in Polynesia in 1960, the Papeete Geophysical Laboratory operated two microbarographs, one at Papeete, and one at Makatea Island, an uplifted atoll 235 km to the Northeast (15.87°S; 146.28°W; Code MKT). Only the MKT record, reproduced on Figure 8a, could be used for this study. Despite ultra-long-period noise at periods on the order of 600 s, it clearly shows a coherent wave train arriving at approximately 02:52 GMT on 23 May 1960, and more apparent on the processed trace plotted on Figure 8b obtained after rectification for clipping (see above) and high-pass filtering at $T \geqslant 600$ s. The characteristics of this wavetrain are a period of 170–195 s, and a zero-to-peak amplitude of approximately 20 dyn/cm^2, or 0.02 mbar; as shown on Figure 8c, the spectral amplitude falls sharply at periods below 160 s. Given the epicentral distance of 7613 km, the group time at MKT is 27,400 s, equivalent to a group velocity $U = 278$ m/s. As shown on Figure 9a, this combination of period and group velocity identifies the wave as an acoustic branch, which in principle could be either S_0 or S_1 (PRESS and HARKRIDER, 1962). The arrival of GR_0, expected 54 mn earlier, could not be recovered. As discussed below, the excitation of the branch S_1

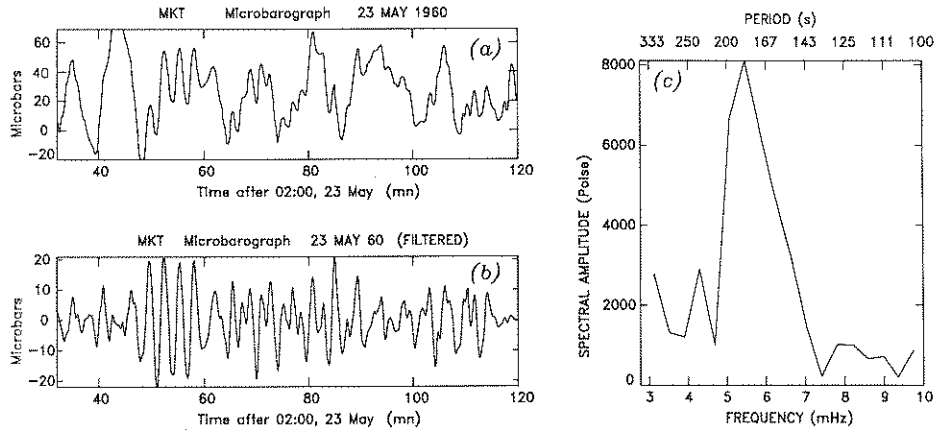

Figure 8

Microbarograph record of the acoustic wave S_0 recorded at Makatea (French Polynesia) from the 1960 Chilean event. (a): Original record. Note strong noise at ultra-long periods, and clipping due to limited dynamic range of graphic recording. (b): Same record after removal of clipping and filtered periods larger than 600 seconds. Note coherent S_0 arrival at 02:52 GMT. (c): Amplitude spectrum of the S_0 wavetrain; note that the energy in the signal is concentrated between 165 and 205 s.

by seismic sources is 2.5 to 5 times smaller than that of S_0 at the periods 170–200 s, and would become comparable (or larger) only at shorter periods ($T < 160$ s), at which the signal has weak amplitudes. We conclude that the wavetrain observed at MKT is indeed part of the S_0 branch. The fact that its group velocity is slightly slower than for a standard model such as ARDC (278 m/s *vs.* 295) probably reflects local geographical conditions (PRESS and HARKRIDER'S (1962) tropical model is significantly slower than ARDC in this range of periods), or perhaps the influence of winds, as documented for example by WEXLER and HASS (1962) in the case of a large 1961 Soviet nuclear explosion.

Table 3 lists the spectral amplitudes at Makatea at the Fourier periods corresponding to the maximum of energy of the wave.

From Overpressure to Seismic Moment

The mantle magnitude philosophy, i.e., obtaining an estimate of the seismic moment M_0 of the source in the absence of any detailed knowledge of the focal mechanism of the event, can be extended conceptually to the case of air-sea coupled waves. Because atmospheric waves can be considered as a superposition of the elasto-gravitational free oscillations of a system consisting of the solid earth, the liquid ocean, and the gaseous atmosphere (conveniently limited at some maximum altitude, on the order of 150 km), the fundamental separation between excitation and propagation effects is maintained, and one expects an equation of the form (1) to hold. Specifically, the moment M_o can be retrieved from the spectral amplitude

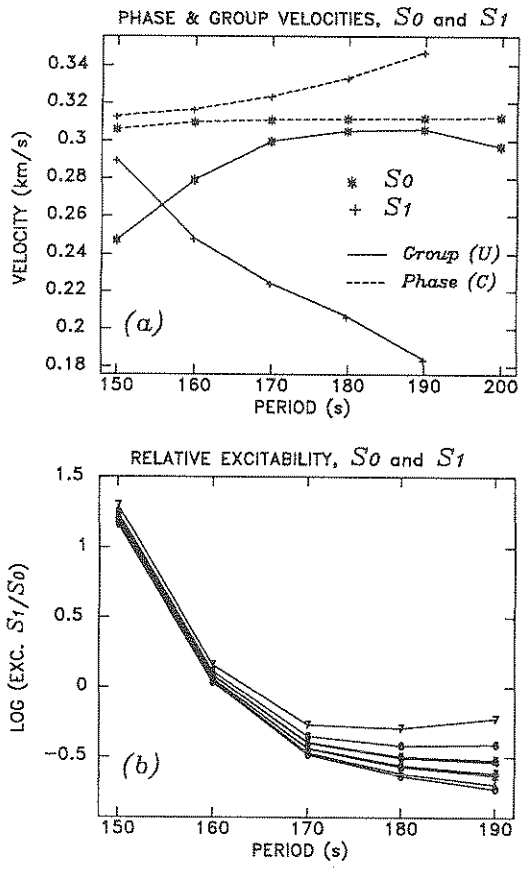

Figure 9
Dispersion properties and relative excitability of the branches S_0 and S_1 in the period range 150–200 s. (a): Theoretical phase and group velocity, detailing the cross-over point between the two branches around 155 s. (b): This frame plots the logarithm of the ratio of the average excitabilities of S_1 and S_0 in the same range of periods. The various curves are relative to sampling depths ranging from 25 km ('0' symbols) to 95 km ('7' symbols). See text for details.

of the pressure disturbance $P(\omega)$ at the surface of the ocean through:

$$M_m = \log_{10} M_o - 20 = \log_{10} P(\omega) + C_D^P + C_S^P + C_0^P. \quad (4)$$

• *Locking constant* C_0^P. As discussed in detail in Paper I, in the case of Rayleigh waves, the correction C_S in (1) was obtained from excitation coefficients K_i computed in units of 10^{-27} dyn^{-1}, since they related ground motion (in cm) to a unit moment of 10^{27} dyn-cm. When $X(\omega)$ was further expressed in μm-s, the constant C_0 took the value -0.90. In the case of pressure waves, we will measure pressures in dyn/cm^2 (10^{-6} bar) and will express the equivalent excitation coefficients K_i^P (see below) in dyn/cm^2 of ocean surface overpressure for the same unit

Table 3

Summary of results for acoustic-gravity waves

Period (s)	Branch	Spectral Amplitude $P(\omega)$, Poise	$\log_{10} P(\omega)$	C_D^P	C_S^P	M_m
		1960 Chile: $M_m^P = 10.51$ (CIFUENTES and SILVER, 1989)				
		Station: Makatea ($\Delta = 7613$ km)				
196.92	S_0	6663.3	3.824	0.160	3.301	10.39
182.86	S_0	8109.3	3.909	0.165	3.351	10.53
170.67	S_0	6314.3	3.800	0.170	3.681	10.75
160.00	S_0	4698.0	3.672	0.175	4.045	10.99
		1964 Alaska: $M_m^P = 9.91$ (KANAMORI, 1977)				
		Station: Berkeley ($\Delta = 3127$ km)				
640.0	GR_0	5564.2	3.745	−0.152	2.198	8.89
512.0	GR_0	3022.8	3.480	−0.150	2.283	8.71
		Station: East San Diego ($\Delta = 3842$ km)				
640.0	GR_0	19317.	4.286	−0.110	2.198	9.47
512.0	GR_0	8843.1	3.947	−0.107	2.283	9.22

moment of 10^{27} dyn-cm, which amounts to measuring K_I^P in units of 10^{-27} cm^{-3}. If $P(\omega)$ is measured in the μbar-s (a unit having dimensions of viscosity, and equivalent to 1 poise or 0.1 Pa-s), the constant C_0 then takes the value $+3.10$.

• *Distance correction* C_D^P. This correction has the same expression as for mantle Rayleigh waves,

$$C_D^P = 0.5 \log_{10} \sin \Delta + \log_{10} e \cdot \frac{\omega \Delta l_{\text{deg}}}{2UQ^P} \tag{5}$$

the only problem being the estimation of the attenuation factor Q^P for pressure waves. In the case of the branch GR_0 at periods of 400–700 s, BOLT and TANIMOTO (1981) have proposed values of Q^P between 2000 and 4000; we will use their "preferred" value of 2000, keeping in mind that, thanks to long periods and short distances, doubling Q^P would affect the final magnitude by at most a few hundredths of one unit.

In the case of S_0 around 170 s, HARKRIDER (pers. comm., 1990) suggests an attenuation coefficient $\gamma = 0.68 \times 10^{-4}$ km^{-1}, equivalent to $Q^P = \pi/TU\gamma = 980$. MIKUMO and BOLT (1985) have proposed a higher value ($Q^P = 1500$). The latter would yield C_D^P at Makatea varying from 0.140 at 160 s to 0.111 at 197 s, while HARKRIDER's stronger attenuation would result in a frequency-independent $C_D^P = 0.209$. In Table 3, we use at each frequency the average between the two values, keeping in mind that the potential error is less than 0.05 units of magnitude.

• *Source excitation correction* C_S^P. In computing this correction, the major effort is to define the equivalent coefficients K_i^P. For this purpose, we use the formalism of HARKRIDER *et al.* (1974), in which the authors merged HARKRIDER'S (1964a) acoustic-gravity wave code and his Rayleigh wave one (HARKRIDER, 1964b) for the purpose of calculating the excitation of (mostly elastic) Rayleigh waves by atmospheric sources. We are interested here in the exact reverse problem, namely the excitation of (mostly atmospheric) air-sea waves by a dislocation source in the solid earth.

HARKRIDER *et al.*'s (1974) code is written in the surface wave formalism, in which the eigenfunction in the solid earth is described in terms of the horizontal and vertical displacements u_x and u_z, and of the tractions σ_{zz} and σ_{xz}. Following OKAL (1982), we can then define excitation coefficients

$$\begin{aligned} K_1^* &= \sigma_{zx}/8\pi c^2 U I^R k\mu \\ K_2^* &= u_x/8\pi c^2 U I^R \\ K_3^* &= \sigma_{zz}/8\pi c^2 U I^R k\mu \\ K_4^* &= u_z/8\pi c^2 U I^R \end{aligned} \tag{6}$$

where the notation is after SAITO (1967): c is the wave's phase velocity, U its group velocity, k its wavenumber, μ the rigidity at the source, and I^R is the Rayleigh energy integral

$$I^R = \int \rho(z)[u_z^2 + u_x^2]\, dz \tag{7}$$

which must now be extended over both earth and atmosphere. OKAL (1982) has shown that, in the limit of a shallow source and for large values of the equivalent order $l = ka - 1/2$, the equivalent normal mode coefficients are given by

$$\begin{aligned} K_1 &= K_1^* \frac{4U}{al} \\ K_2 &= K_2^* \frac{4U}{al^2} \\ K_0 &= \frac{4U}{al} \cdot 2 \cdot \frac{3\lambda + 2\mu}{\lambda + 2\mu} \left[K_4^* - \frac{a}{3\lambda + 2\mu} K_3^* - \tfrac{1}{2} K_2^* \right]. \end{aligned} \tag{8}$$

The final step in computing the coefficients K_i^P is to scale the K_i's by the ratio of the overpressure at the surface of the ocean to the vertical displacement at its bottom, which is usually normalized to 1 in HARKRIDER *et al.*'s (1974) code. The equivalence of the two formalisms was checked numerically by computing a standard 100-second mantle Rayleigh wave both using our normal mode algorithm, and as a particular case of a coupled air-sea wave using these authors' code.

From there on, the computation proceeds exactly as in Paper I. In the absence of any detailed knowledge of the focal geometry, the excitation terms are averaged over a large number of double-couple geometries, and the logarithmic average excitability computed as a function of frequency. However, in the case of acoustic-gravity waves, the influence of depth can become significant, and must be further discussed. This can be understood since the eigenfunction is expected to be primarily an elastic wave in the solid earth; its potentials (compressional and shear) will satisfy their respective wave equation and their "skin depths" δ_α and δ_β will be given by

$$\frac{1}{\delta_\alpha^2} = \omega^2\left[\frac{1}{c^2} - \frac{1}{\alpha^2}\right]; \quad \frac{1}{\delta_\beta^2} = \omega^2\left[\frac{1}{c^2} - \frac{1}{\beta^2}\right]. \tag{9}$$

In the limit when the phase velocity c, controlled by the atmospheric part of the wave, is very small compared to α or β, $\delta = c/\omega = \Lambda/2\pi$, where Λ is the wavelength. OKAL (1988) used a similar argument to explain that tsunami excitation had in general little dependence on depth. In this respect, the case of the gravity and acoustic branches will be significantly different. For the GR_0 branch, the large period (up to 650 s) will offset the effect of the small phase velocity, and the resulting wavelength $\Lambda = 200$ km will be large enough to minimize the influence of depth on excitation, at least for $h \leqslant 75$ km, as shown on Figure 10a. We will use a typical depth of 60 km, corresponding to the probable centroid of the Alaskan event, but the figure shows clearly that the effect of depth should be minimal.

On the other hand in the case of the acoustic modes at shorter periods, the wavelength will be on the order of 50 km, resulting therefore in substantial dependence of excitation on depth. Figure 10b shows the variation of the logarithmic average excitability with depth for the mode S_0 in the relevant period range. In the case of the Chilean earthquake, we will use a depth of 65 km, which can be taken to represent the centroid of the "mainshock" part of this event, but we must keep in mind that our results will remain somewhat depth-dependent.

Results

The resulting values of M_m, computed from Equation (4), are listed in the last column of Table 3. To our knowledge, these results constitute the first time that acoustic-gravity waves have been used to infer the size ("moment") of a major earthquake, although MIKUMO (1968) did forward-model the Alaskan GR_0 records. The single barograph record at MKT provides an excellent estimate for the Chilean event. Despite the substantial influence of depth (which in a real time situation might not be available accurately), the exceptional size of the event is established beyond doubt. It could be argued from Figure 10b that a shallower focus (say, 30 km) would result in a significantly smaller moment (by about one order of magnitude); however, at several times 10^{29} dyn-cm, the event would still be gigantic.

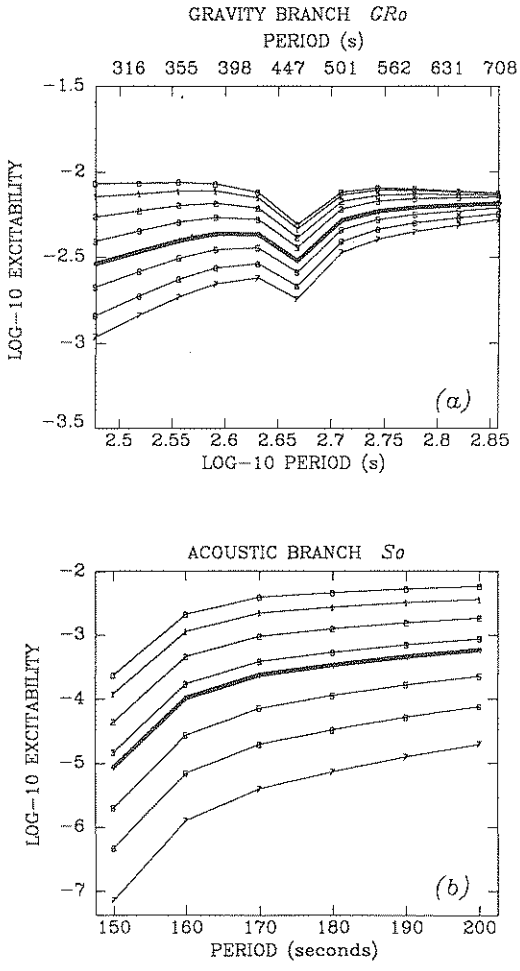

Figure 10

Logarithmic average excitability of the branches GR_0 (*Top;* in the range $T = 300$–700 s), and S_0 (*Bottom;* in the vicinity of $T = 175$ s). This figure is comparable to Figure 3 of Paper I. Note that the two frames use different scales; see text for details.

Furthermore, due in part to scaling relations for large subduction zone earthquakes, there exists a trade-off between source shallowness and size: the very biggest earthquakes are known to involve significant down-dip rupture with centroids extending to 50–60 km on shallow dipping planes, deeper on steep ones. As a result, there is no possibility of explaining the S_0 spectral amplitudes at MKT with anything short of a mammoth event of at least 10^{30} dyn-cm.

In the case of the GR_0 records from the Alaskan earthquake, the resulting M_m values are significantly deficient, especially at BKS. We investigated the effect of the focal-receiver geometry, by computing a "corrected" magnitude M_c, as in the case

of seismic waves, but this can account for only 0.1 to 0.25 units. We believe on the other hand that the deficiency observed at Berkeley and East San Diego is a consequence of drastic directivity effects.

Effect of Directivity

As discussed by BEN-MENAHEM (1961) in the case of seismic surface waves, and BEN-MENAHEM and ROSENMAN (1972) in the case of tsunami waves, directivity is controlled by a supplemental contribution $D(\phi)$ which must be multiplied into the spectral amplitude:

$$D(\phi) = \text{sinc } Y = \frac{\sin Y}{Y} \quad \text{with} \quad Y = \frac{\omega L}{2c} \cdot \left[\frac{c}{V_R} - \cos \phi \right] \tag{10}$$

where L is the length of the fault, V_R the rupture velocity, and ϕ the azimuth to the station relative to the direction of rupture. For any given source size, $D(\phi)$ goes to 1 as $\omega \to 0$, but its azimuthal pattern can vary considerably with the type of wave. BEN-MENAHEM and ROSENMAN (1972) have shown that the maximum of D ($Y = 0$) occurs in the direction of faulting for "fast" waves traveling at a phase velocity close to V_R, but at right angles to that direction for "slow" waves, such as tsunamis and acoustic-gravity waves. In addition, the width of the directivity lobes is controlled by the second derivative $d^2D(\phi)/d\phi^2$, which in the vicinity of $Y = 0$ behaves like

$$-\tfrac{1}{3}\left(\frac{dY}{d\phi}\right)^2 - \frac{Y}{3}\frac{d^2Y}{d\phi^2} = -\tfrac{1}{3}\left(\frac{\omega L}{2c}\right)^2 \sin^2\phi = -\frac{\pi^2}{3}\frac{L^2}{\Lambda^2}\sin^2\phi. \tag{11}$$

For a fast wave, the maximum of directivity takes place in the direction of rupture ($\phi = 0$), where the second derivative is zero, and the lobe is well developed. For a slow wave, $\phi = \pi/2$ at the lobe, and the lobe is narrow. This effect is further controlled by the term $(L/\Lambda)^2$, resulting in even narrower lobes for the air wave than for the tsunami. These results are summarized on Figure 11, in which we computed directivity coefficients using KANAMORI'S (1970) rupture parameters ($L = 600$ km; $\phi_R = 205°$; $V_R = 3.5$ km/s) for the Alaskan earthquake. The top trace involves a period $T = 200$ s and a phase velocity $c = 4.6$ km/s, values characteristic of both Love and Rayleigh mantle waves. The bottom figure is for slow waves: a tsunami (solid line), and a gravity wave of period 400 s (dashed line). In the latter case, the principal lobe is very narrow, and the secondary ones have all but disappeared.

Fortunately, in the 1960 Chile-to-Makatea geometry, the station azimuth is within 3 degrees of the direction of maximum $D(\phi)$, and directivity effects can be neglected. In the case of the 1964 Alaska records, we computed $D = 0.57$ ($T = 640$ s) and $D = 0.38$ ($T = 512$ s) at ESD; $D = 0.36$ ($T = 640$ s) and $D = 0.14$ ($T = 512$ s) at BKS. When corrected for, these terms bring the magnitude estimates

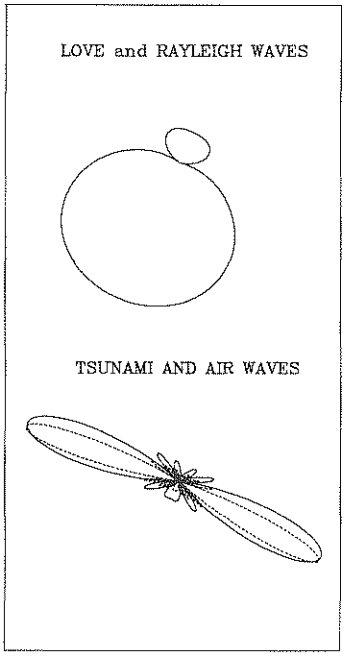

Figure 11
Directivity functions $D(\phi)$ computed in the rupture geometry of the Alaskan earthquake, as given by KANAMORI (1970). *Top:* Seismic surface waves ($T = 200$ s; $c = 4.6$ km/s); this case describes both Rayleigh and Love waves. *Bottom:* The solid line illustrates tsunami waves ($T = 1000$ s; $c = 220$ m/s), the dashed one gravity waves in the atmosphere ($T = 400$ s; $c = 310$ m/s).

up to 9.71, 9.64, 9.33 and 9.58, respectively, which are much closer to the published values 9.88 (KANAMORI, 1970) and 9.91 (KANAMORI, 1977).

In conclusion of this section, the spectral amplitudes of acoustic-gravity waves generated by gigantic earthquakes can be used to provide estimates of M_0, through an algorithm similar to that of the mantle magnitude M_m. However, the combination of slow phase velocities and relatively short wavelengths gives rise to drastic directivity effects which will result in generally deficient estimates.

Conclusions

The principal conclusions of this study can be summarized as follows:

1. The mantle magnitude M_m does successfully recognize truly gigantic earthquakes, with a level of performance comparable to that achieved on more recent digital data sets. These results provide a necessary complement at very large moments to the studies reported at lower magnitudes in Papers I and II and in

REYMOND *et al.* (1991). The fact that no saturation of the magnitude scale takes place, even for the largest events ever recorded instrumentally, provides a full *a posteriori* justification to the endeavor of developing the mantle magnitude scale M_m.

2. Even M_m measurements effected in less-than-favorable operational conditions can yield reasonable estimates of the seismic moment. These would include instruments with a strongly inadequate response in the frequency range of mantle waves, and records severely clipped due to the mechanical limitations of paper recorders. Microbarograph records of air-coupled Rayleigh waves also yield reliable estimates.
3. In the case of the very largest events capable of exciting the acoustic-gravity modes of the atmosphere, the basic philosophy of the mantle magnitude approach can be extended to these waves, and an estimate of M_0 can be retrieved from the spectral amplitudes of the overpressure signal at the earth's surface. However, relative to regular seismic mantle waves, these calculations are more sensitive to such effects as true source depth (especially in the case of the acoustic modes such as S_0), and directivity induced by source finiteness. Nevertheless, the air wave signals can be used to recognize the truly exceptional size of the 1960 and 1964 events.

Acknowledgments

We are grateful to our colleagues at Palisades, Uppsala and Pasadena for the use of their archive facilities. We thank David Harkrider for lending us his air-sea-solid earth wave codes, and for many discussions on atmospheric waves. This research was supported by Commissariat à l'Energie Atomique (France), and the National Science Foundation, under Grant EAR-87-20547.

REFERENCES

BENIOFF, H., EWING, M., and PRESS, F. (1951), *Sound Waves in the Atmosphere Generated by a Small Earthquake*, Proc. Natl. Acad. Sci. U.S. *37*, 600–603.

BEN-MENAHEM, A. (1961), *Radiation of Seismic Surface Waves from Finite Moving Sources*, Bull. Seismol. Soc. Amer. *51*, 401–435.

BEN-MENAHEM, A. (1971), *The Force System of the Chilean Earthquake of 1960 May 22*, Geophys. J. Roy. Astr. Soc. *25*, 407–417.

BEN-MENAHEM, A., and ROSENMAN, M. (1972), *Amplitude Patterns of Tsunami Waves from Submarine Earthquakes*, J. Geophys. Res. *77*, 3097–3128.

BOLT, B. A. (1964), *Seismic Air Waves from the Great Alaskan Earthquake*, Nature *202*, 1095–1096.

BOLT, B. A., and TANIMOTO, T. (1981), *Atmospheric Oscillations after the May 18, 1980 Eruption of Mount St. Helens*, EOS, Trans. Amer. Geophys. Un. *62*, 529–530.

BRUNE, J. N., and ENGEN, G. R. (1969), *Excitation of Mantle Love Waves and Definition of Mantle Wave Magnitude*, Bull. Seismol. Soc. Amer. *59*, 923–933.

CIFUENTES, I. L., and SILVER, P. G. (1989), *Low Frequency Source Characteristics of the Great 1960 Chilean Earthquake*, J. Geophys. Res. *94*, 643–663.

DONN, W. L., and POSMENTIER, E. S. (1964), *Ground-coupled Air Waves from the Great Alaskan Earthquake*, J. Geophys. Res. *69*, 5357–5361.

DZIEWONSKI, A. M., and GILBERT, J. (1972), *Observations of Normal Modes from 84 Records of the Alaskan Earthquake of 1964 March 28*, Geophys. J. Roy. Astr. Soc. *27*, 393–446.

DZIEWONSKI, A. M., FRIEDMAN, A., GIARDINI, D., and WOODHOUSE, J. H. (1983), *Global Seismicity of 1982: Centroid Moment Tensor Solutions for 308 Earthquakes*, Phys. Earth Planet. Inter. *33*, 76–90.

GELLER, R. J. (1976), *Scaling Relations for Earthquake Source Parameters and Magnitudes*, Bull. Seismol. Soc. Amer. *66*, 1501–1523.

GELLER, R. J., *I. Earthquake source models, magnitudes and scaling relations. II. Amplitudes of rotationally split normal modes for the 1960 Chilean and 1964 Alaskan earthquakes*, Ph.D. Thesis (Calif. Inst. Technol., Pasadena 1977), 211 pp.

GELLER, R. J., and KANAMORI, H. (1977), *Magnitude of Great Shallow Earthquakes from 1904 to 1952*, Bull. Seismol. Soc. Amer. *67*, 587–598.

GUTENBERG, B., and RICHTER, C. F., *Seismicity of the Earth and Associated Phenomena* (Princeton University Press 1954), 2nd edition, 310 pp.

HARKRIDER, D. G. (1964a), *Theoretical and Observed Acoustic-gravity Waves from Explosive Sources in the Atmosphere*, J. Geophys. Res. *69*, 5295–5321.

HARKRIDER, D. G. (1964b), *Surface Waves in Multilayered Elastic Media, I. Rayleigh and Love Waves from Buried Sources in a Multilayered Elastic Half-space*, Bull. Seismol. Soc. Amer. *54*, 627–679.

HARKRIDER, D. G., NEWTON, C. A., and FLINN, E. A. (1974), *Theoretical Effect of Yield and Burst Height of Atmospheric Explosions on Rayleigh Wave Amplitudes*, Geophys. J. Roy. Astr. Soc. *36*, 191–225.

HASKELL, N. A. (1951), *A Note on Air-coupled Surface Waves*, Bull. Seismol. Soc. Amer. *41*, 295–300.

KANAMORI, H. (1970), *The Alaska Earthquake of 1964: Radiation of Long-period Surface Waves and Source Mechanism*, J. Geophys. Res. *75*, 5029–5040.

KANAMORI, H. (1977), *The Energy Release in Great Earthquakes*, J. Geophys. Res. *82*, 2981–2987.

KANAMORI, H., and ANDERSON, D. L. (1975), *Amplitude of the Earth's Free Oscillations, and Long-period Characteristics of the Earthquake Source*, J. Geophys. Res. *80*, 1075–1078.

KANAMORI, H., and CIPAR, J. J. (1974), *Focal Process of the Great Chilean Earthquake May 22, 1960*, Phys. Earth Planet. Inter. *9*, 128–136.

KULHÁNEK, O., *The status, importance and use of historical seismograms in Sweden*, In *Historical Seismograms and Earthquakes of the World* (Lee, W. H. K., Meyers, H., and Shimazaki, K. eds) (San Diego, Academic Press 1987), pp. 64–69.

MIKUMO, T. (1968), *Atmospheric Pressure Waves and Tectonic Deformation Associated with the Alaskan Earthquake of March 28, 1964*, J. Geophys. Res. *73*, 2009–2025.

MIKUMO, T., and BOLT, B. A. (1985), *Excitation Mechanism of Atmospheric Pressure Waves from the 1980 Mount St. Helens Eruption*, Geophys. J. Roy. Astr. Soc. *81*, 445–461.

OKAL, E. A. (1982), *Higher Moment Excitation of Normal Modes and Surface Waves*, J. Phys. Earth *30*, 1–31.

OKAL, E. A. (1988), *Seismic Parameters Controlling Far-field Tsunami Amplitudes: A Review*, Natural Hazards *1*, 67–96.

OKAL, E. A. (1989), *A Theoretical Discussion of Time-domain Magnitudes: The Prague Formula for M_s and the Mantle Magnitude M_m*, J. Geophys. Res. *94*, 4194–4204.

OKAL, E. A. (1991), *M_m: Use of a Mantle Magnitude for the Reassessment of the Seismic Moment of Historical Earthquakes, 1905–1964*, Pure Appl. Geophys., submitted.

OKAL, E. A., and TALANDIER, J. (1989), *M_m: A Variable Period Mantle Magnitude*, J. Geophys. Res. *94*, 4169–4193.

OKAL, E. A., and TALANDIER, J. (1990), *M_m: Extension to Love Waves of the Concept of a Variable-period Mantle Magnitude*, Pure Applied Geophys. *134*, 355–384.

PRESS, F., and HARKRIDER, D. G. (1962), *Propagation of Acoustic-gravity Waves in the Atmosphere*, J. Geophys. Res. *67*, 3889–3908.

REYMOND, D., HYVERNAUD, O., and TALANDIER, J. (1991), *Automatic Detection, Location and Quantification of Earthquakes: Application to Tsunami Warning*, Pure Appl. Geophys. *135*, 361–382.

RITSEMA, A. R. (1980), *Observations of St. Helens Eruption*, EOS, Trans. Amer. Geophys. Un. *61*, 1202.

SAITO, M. (1967), *Excitation of Free Oscillations and Surface Waves by a Point Source in a Vertically Heterogeneous Medium*, J. Geophys. Res. *72*, 3689–3699.

TALANDIER, J., and OKAL, E. A. (1989), *An Algorithm for Automated Tsunami Warning in French Polynesia, Based on Mantle Magnitudes*, Bull. Seismol. Soc. Amer. *79*, 1177–1193.

WEXLER, H., and HASS, W. A. (1962), *Global Atmospheric Pressure Effects of the October 30, 1961, Explosion*, J. Geophys. Res. *67*, 3875–3887.

YUEN, P. C., WEAVER, P. F., SUZUKI, R. K., and FURUMOTO, A. S. (1969), *Continuous, Traveling Coupling between Seismic Waves and the Atmosphere Evident in May 1968 Japan Earthquake Data*, J. Geophys. Res. *74*, 2256–2264.

(Received February 6, 1991, accepted May 18, 1991)